Mxi1-0, an Alternatively Transcribed Mxi1 Isoform, Is Overexpressed in Glioblastomas

Lars D. Engstrom, Andrew S. Youkilis, Judith L. Gorelick, Datong Zheng, Valerie Ackley, Christy A. Petroff, Linda Q. Benson, Melissa R. Coon, Xiaoxiang Zhu, Samir M. Hanash and Daniel S. Wechsler

Section of Pediatric Hematology-Oncology, Department of Pediatrics and Communicable Diseases, The University of Michigan School of Medicine, Ann Arbor, MI, USA

Abstract

The c-Myc transcription factor regulates expression of genes related to cell growth, division, and apoptosis. Mxi1, a member of the Mad family, represses transcription of c-Myc–regulated genes by mediating chromatin condensation via histone deacetylase and the Sin3 corepressor. Mxi1 is a c-Myc antagonist and suppresses cell proliferation *in vitro*. Here, we describe the identification of Mxi1-0, a novel Mxi1 isoform that is alternatively transcribed from an upstream exon. Mxi1-0 and Mxi1 have different amino-terminal sequences, but share identical Max- and DNA-binding domains. Both isoforms are able to bind Max, to recognize E-box binding sites, and to interact with Sin3. Despite these similarities and in contrast to Mxi1, Mxi1-0 is predominantly localized to the cytoplasm and fails to repress c-Myc–dependent transcription. Although Mxi1-0 and Mxi1 are coexpressed in both human and mouse cells, the relative levels of Mxi1-0 are higher in primary glioblastoma tumors than in normal brain tissue. This variation in the levels of Mxi1-0 and Mxi1 suggests that Mxi1-0 may modulate the Myc-inhibitory activity of Mxi1. The identification of Mxi1-0 as an alternatively transcribed Mxi1 isoform has significant implications for the interpretation of previous Mxi1 studies, particularly those related to the phenotype of the *mxi1* knockout mouse.

Neoplasia (2004) **6**

Keywords: Mxi1, Myc, chromosome 10, alternative transcript, glioblastoma.

Introduction

The Myc family of transcription factors has been implicated in the pathogenesis of a variety of cancers. Myc contributes to enhanced proliferation and tumorigenesis by multiple mechanisms, and recent studies have indicated a key role for Myc-dependent transcriptional activation and repression of genes necessary for proliferation and survival [1–4]. The identification of the Mad family of Myc antagonists (Mad1, Mxi1, Mad3, Mad4, Rox/Mnt, Mga) led to the recognition that the regulation of genes by Myc is complex [5–10]. Numerous studies have demonstrated the ability of Mad proteins to counteract the ability of Myc to transform cells, as well as to reduce Myc-dependent transactivation (reviewed in Refs. [11–14]). Whereas Mad proteins recruit histone deacetylase to actively repress transcription, the precise means by which Mad proteins regulate Myc activity, as well as their role in the normal differentiation process, remain unclear. The specific features that distinguish the function of individual Mad family members from each other are also unknown.

Mxi1 was initially identified as a heterodimeric partner for Max using the yeast-two hybrid system [6]. The human *MXI1* gene is located on chromosome 10q24–q25 [15,16] and is composed of six exons (roughly corresponding to Mxi1 functional domains) that span >60 kb [17]. The ability of Mxi1 to interact with the Sin3 corepressor results in recruitment of histone deacetylase to the promoters of regulated genes, with consequent chromatin condensation and transcriptional repression [18–22]. Numerous studies have demonstrated the ability of Mxi1 to counteract Myc-dependent transcription and transformation, and overexpression of Mxi1 results in growth arrest [6,23–25]. The possibility that *MXI1* is a tumor suppressor gene (by virtue of its antagonism of Myc) is supported by the tumor-prone phenotype of the *mxi1* knockout mouse [26]. However, only a small fraction of prostate and neurofibrosarcoma tumors have been shown to harbor *MXI1* coding sequence mutations [27–29]. A recent study indicates that Mxi1 may regulate a set of genes distinct from those regulated by Myc [30]. The precise mechanisms by which Mxi1 produces its repressive effects and the interplay among the various Mad family members remain to be clarified.

After the discovery of human *MXI1* [6], several groups independently identified *mxi1* homologues in the mouse. Shapiro et al. [15] first mapped the mouse *mxi1* locus to chromosome 19, a region syntenic with human chromosome 10q. Subsequently, Schreiber-Agus et al. [19] described a mouse Mxi1 isoform (hereafter referred to as mMxi1) whose amino acid sequence was essentially identical to human Mxi1 (hMxi1), except for minor C-terminal residue differences (Figure 1*A*).

Abbreviations: RT-PCR, reverse transcription–polymerase chain reaction; IP, immunoprecipitation; WCL, whole cell lysate; HA, hemagglutinin; SID, Sin3 interaction domain

Address all correspondence to: Daniel S. Wechsler, Section of Pediatric Hematology-Oncology, The University of Michigan, 1500 East Medical Center Drive, CCGC 4312, Ann Arbor, MI 48109-0936. E-mail: dwechsl@umich.edu

Received 19 March 2004; Revised 14 June 2004.

DOI 10.1593/neo.04244

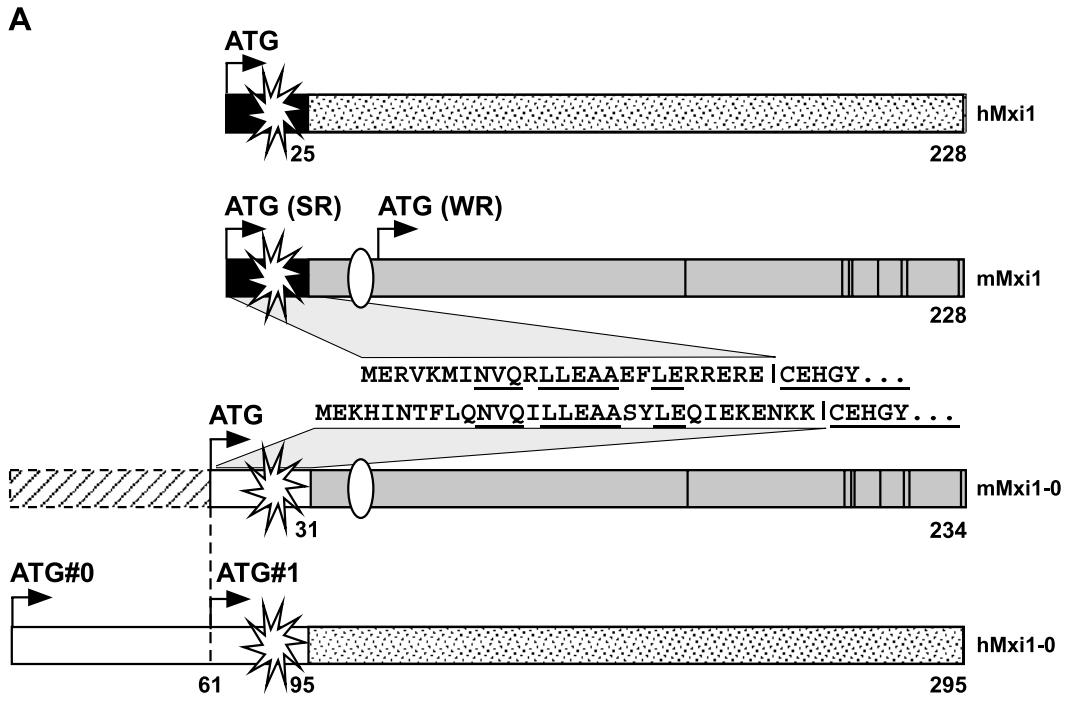

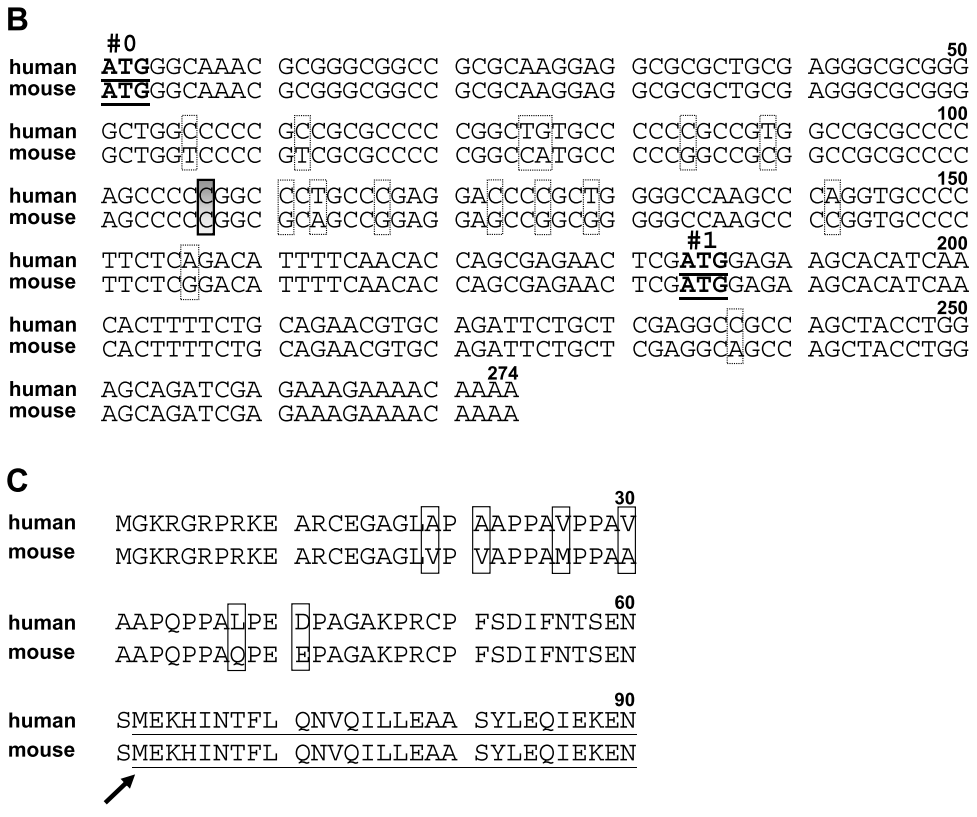

Figure 1. *(A) Identification of different human (h) and mouse (m) Mxi1 isoforms. Bars represent sequences encoded by exons 2 to 6 in human (hatched) and mouse (shaded) isoforms. Vertical bars in the mMxi1 forms indicate single amino acid (aa) differences from hMxi1. Solid black bars are derived from exon 1 sequence and open white bars from exon 0 sequence. Start codons (ATG) and aa numbers are shown above and below bars, respectively. Start codons corresponding to the strong (SR) and weak repressor (WR) isoforms of mouse Mxi1 [19] are indicated. The location of the Sin3 interaction domain (SID) in both exon 0– and exon 1–encoded sequences is shown as an open star. Exon 1 and partial exon 0 aa sequences are indicated below mMxi1-1 and above mMxi1-0, respectively, with residues common to both underlined. Common exon 2 sequence follows vertical bars in these sequences. The crosshatched dashed rectangle upstream of ATG in mMxi1-0 indicates extent of novel sequence encoded by exon 0. Ovals indicate the location of sequence encoded by disrupted exon 2 in the mxi1 knockout [26]. (B) Comparison of human and mouse exon 0 nucleotide sequences. Significant homology is observed between human (GenBank Accession No. AL360182) and mouse (GenBank Accession No. NT_039692) sequences, with differences indicated by hatched rectangles. The shaded rectangle indicates the location of the cytosine residue that was absent from the Shimizu et al. [31] mMxi1-0 sequence, the presence of which permits an open reading frame from ATG #0 (underlined). Originally defined ATG#1 start codon from mMxi1-0 is also underlined. (C) Comparison of human and mouse exon 0–encoded amino acid sequences. Again, significant homology is observed, with differences indicated by rectangles. Sequence common to that predicted by Shimizu et al. [31] is underlined, with initial methionine indicated by arrow.*

Like hMxi1, this mMxi1 isoform was able to repress transcription (SR, strong repressor) and antagonize c-Myc–dependent transformation. Of note, this group described a second mouse Mxi1 variant with distinct transcriptional repressive abilities—the so-called weak repressor (WR)—that differed only in the absence of the exon 1–encoded SID. The presence of a cryptic ATG in exon 2 of mouse *mxi1* could account for the absence of the SID in the WR isoform. At the same time, Shimizu et al. [31] identified an alternative mouse Mxi1 isoform (subsequently referred to here as mMxi1-0) that was identical to mMxi1-1 in its C terminus, but differed substantially in its initial N-terminal amino acid sequence (Figure 1*A*). No specific information related to the functional activity of mMxi1-0 has been reported, and only a single subsequent reference has been made to mMxi1-0 [32]. The discrepancy between the two mouse *mxi1* forms has not been reconciled in the literature.

We have recently discovered hMxi1-0, an isoform of Mxi1 translated from an alternative transcript derived from a promoter upstream of a previously unidentified exon (exon 0) at both the human *MXI1* and mouse *mxi1* loci. hMxi1-0 shares significant homology with mMxi1-0, indicating cross-species conservation. Intriguingly, hMxi1-0 is expressed at relatively higher levels in tumor cells compared with normal tissues. Functional analysis of hMxi1-0 indicates that whereas it is able to heterodimerize with Max and recruit Sin3, it lacks the ability of Mxi1 to repress Myc-dependent transcription. The recognition that the same locus yields protein products with distinct activities represents a novel mechanism by which the repressive activity of Mxi1 might be attenuated or antagonized in the absence of somatic mutation within Mxi1 coding exons. This finding has implications for regulation of the activity of other Myc/Mad family members and also for the published phenotype of the *mxi1* knockout mouse.

Materials and Methods

Plasmid Construction

MXI1-0 and *MXI1* cDNAs were amplified from a human heart cDNA library (BD Biosciences-Clontech, Palo Alto, CA) using *Bam*H1 sequence containing forward primers (5′-CGGGATCCCATGGGCAAACGCGGGCGG-3′ and 5′-CGCGGATCCTCTAGACCATGGAGC GGGTGAAGATGATC-3′, respectively), and a reverse primer (5′-CGCGGATCCTTAAGCGT AGTCTGGGACGTCGTATGGGTACAAGCTTGAAGTGAATGAAAGTTTGAC-3′) that includes coding sequence for an influenza hemagglutinin (HA) peptide epitope (YPYDVPDYA). This HA tag permits detection of either Mxi1-0-HA or Mxi1-HA using anti–HA antibodies (Santa Cruz Biotechnology, Santa Cruz, CA, and Roche, Indianapolis, IN). The *MXI1-0*-HA and *MXI1*-HA cDNAs were subcloned into the following: 1) the pcDNA3.1 eukaryotic expression vector (Invitrogen, Carlsbad, CA); 2) the pIRES2-EGFP eukaryotic expression vector (BD Biosciences-Clontech); and 3) the pET-30a(+)vector (Novagen, San Diego, CA) for preparation of purified 6xHistidine-tagged protein in bacteria. DNA fragments corresponding to sequences unique to exon 0 and exon 1 were also subcloned into pBluescript KS– (Stratagene, La Jolla, CA) to permit generation of exon 0– and exon 1–specific RNA probes.
An *Xho*I/*Nco*I DNA fragment containing 1000 bp of genomic sequence upstream of the *MXI1-0* ATG#0 was cloned into the pGL3-Basic luciferase vector (Promega, Madison, WI) in both forward (pGL3Basic-Ex0P) and reverse (pGL3Basic-Ex0PRev) orientations for transcription studies. Similar constructs containing 435 and 145 bp were prepared using *Apa*L1/*Nco*I and *Pst*I/*Nco*I fragments, respectively. The pGLDH637Luc luciferase reporter (a Myc-responsive, E-box-containing LDH promoter-luciferase reporter plasmid [33]) and pRSV-Myc expression plasmids were a gift of C. Dang (Baltimore, MD). pCMV-Max-YFP-FLAG was a gift of Tom Kerppola (Ann Arbor, MI), and pCS2+MT-mSin3A was a gift of Don Ayer (Salt Lake City, UT). DNA sequencing was performed to confirm appropriate sequence and orientation of each plasmid vector. Sequencing was performed using the fluorescent dideoxy terminator method of cycle sequencing on a PE/ABd 373a automated DNA sequencer following ABd protocols at the University of Michigan DNA Sequencing Core.

Cell Culture

U87MG and U373MG glioblastoma cells (ATCC, Manassas, VA) were maintained in Eagle's minimum essential medium (EMEM) supplemented with 10% FBS, penicillin/streptomycin and L-glutamine. K562 cells were passaged in RPMI 1640 with 10% FBS with additives. NIH3T3 fibroblasts and COS7 cells were maintained in Dulbecco's modified Eagle's medium (DMEM) with 10% FBS with additives.

Restriction Landmark Genome Scanning

Restriction landmark genome scanning [34–36] was performed using IMR-32 human neuroblastoma cells as described previously [37,38].

Genome Analysis

A P1 clone derived from human chromosome 10 and including the *MXI1* locus was obtained from Genome Systems Inc. (St. Louis, MO) after screening with *MXI1-0*– and *MXI1*-specific primer pairs. Southern blot analysis was performed with digoxigenin-labeled probes (Roche) after restriction digestion with multiple enzymes according to standard protocols. Chromatograms of sequences were analyzed both visually and using MacVector 6.5.3 with AssemblyLIGN (Accelrys, San Diego, CA). A BLAST search identified a human chromosome 10 genomic sequence that included exon 0 (GenBank Accession No. AL360182), and each of the *MXI1* exons 0 to 6 was matched up with this sequence using MacVector to identify interexon distances. Similarly, mouse chromosome 19 genomic sequence (GenBank Accession No. NT_039692) was also found to contain *mxi1* exons 0 to 6.

Luciferase Assays

To evaluate transcription through the *MXI1-0* promoter, transfections were performed as previously described [39] in hematopoietic K562 cells, as well as U87MG and U373MG

glioblastoma cell lines. K562 cells growing in log phase were washed with ice-cold Opti-MEM (Invitrogen) and resuspended in Opti-MEM at a concentration of 5×10^7/ml. A total of 1×10^7 cells were incubated with 5 μg of pGL3Basic-Ex0P, pGL3Basic-Ex0PRev, or pGL3-Basic-Ex1P promoter luciferase plasmids and 50 ng of pRL-TK *Renilla* vector (Promega) at room temperature for 10 minutes. Cells were transfected by electroporation with a BTX Electro Cell Manipulator 600 at 350 V, 650 μF, and 13 Ω. Cells were then incubated at room temperature for 15 minutes and transferred to 3 ml of prewarmed (37°C) RPMI 1640 medium with additives. The transfected cells were maintained in 5% CO_2 at 37°C for 18 h, at which time they were harvested, and both luciferase and *Renilla* activity were measured on a Monolight 3010 luminometer (BD Biosciences Pharmingen, San Diego, CA) using the Dual-Luciferase assay system (Promega). Luciferase (L) activity values were normalized to the *Renilla* (R) activities for each sample (L/R), and reported relative to pGL3-Basic-*MXI1* (100%). All reactions were performed in triplicate and repeated at least three times; results are expressed as the mean ± SEM. U87MG and U373MG cells were electroporated at 175 V, 850 μF, and 72 Ω, transferred to EMEM, and subsequently treated as described for K562 cells.

Northern Blot Analysis

Single-stranded RNA probes specific to *MXI1-0* and *MXI1* were generated by reverse transcription from pBluescript plasmids containing either exon 0 or exon 1, and end-labeled with ^{33}P. Premade multiple tissue fetal and adult Northern blots (Invitrogen) were probed according to the manufacturer's instructions. Autoradiographs were obtained at 48 hours.

Multiplex RT-PCR Assay

An *MXI1*/*MXI1-0*–specific multiplex, one-step reverse transcription–polymerase chain reaction (RT-PCR) assay (Access RT-PCR, Promega) was set up using separate forward primers for exon 0 (5′-GACATTTTCAACACCAGCGAGAA CTCGATG-3′) and exon 1 (5′-CAACGTGCAGCGTCTGCTGGAGGC-3′) and a common reverse primer from exon 3 (5′-CGATTCTTTTCCAGCTCATTGTG-3′) (Figure 4*B*). Two hundred nanograms of total RNA was used for the template. Reverse transcription was performed for 45 minutes at 48°C, followed by 35 cycles of: denaturation (94°C for 30 seconds), annealing (58°C for 1 minute), and extension (68°C for 2 minutes), with a final 7-minute, 68°C extension. A Perkin-Elmer GeneAmp PCR System 2400 was used for amplification. The expected product sizes for Mxi1-0 and Mxi1 are 281 and 216 bp, respectively. Quantitation of band intensity was performed using KODAK 1D Image Analysis Software (Rochester, NY).

Immunofluorescence

COS7 cells were transiently transfected with pIRES2-EGFP-*MXI1*-HA or pIRES2-EGFP-*MXI1-0*-HA using FuGENE 6 (Roche). Forty-eight hours later, cells were permeabilized with 0.02% saponin in Buffer A (150 mM KCl, 2 mM $MgCl_2$, 20 mM HEPES, 1 mM EGTA, 1 mM EDTA, 10% glycerol) for 15 minutes at 4°C, fixed with 100% methanol for 5 minutes at −20°C, and then stained with 1:200 primary rabbit anti–HA antibody (Roche) followed by Cy3-conjugated 1:400 secondary goat anti–rabbit antibody (Jackson ImmunoResearch Laboratories, West Grove, PA). Cells were visualized with a CoolSnap Pro CCD camera (Media Cybernetics, Carlsbad, CA) on a Nikon Eclipse E600 microscope or a Zeiss LSM510 confocal microscope.

In Vitro Transcription/Translation and Western Blot Analysis

pcDNA3.1-*MXI1-0*-HA or pcDNA3.1-*MXI1*-HA plasmids were used in the TNT T7 Quick Coupled Transcription/Translation System (Promega) according to the manufacturer's instructions. ^{35}S-methionine labeling and Western blot analysis were used for protein detection. For Western blots, cell lysates were subjected to three freeze-thaw cycles, sonicated, normalized for total protein concentration, mixed with equal volumes of 2 × loading buffer, and boiled for 10 minutes at 95°C. Samples were separated on a 12% acrylamide SDS gel, followed by transfer to a polyvinylidene fluoride (PVDF) membrane (Bio-Rad, Hercules, CA). HA-tagged proteins were detected with a rabbit polyclonal anti–HA antibody (Santa Cruz Biotechnology), followed by goat anti–rabbit IgG HRP (Jackson ImmunoResearch Laboratories). An HA-tagged Bcl-x_S protein (gift of G. Nunez) was used as a positive control for the HA antibody, and an expected band of approximately 22 kDa was observed (data not shown). FLAG-tagged Max was detected with either mouse anti–FLAG antibody (Sigma, St. Louis, MO) or mouse anti-Max antibody (Santa Cruz Biotechnology), and Myc-tagged mSin3A was detected with rabbit anti–c-Myc antibody (Santa Cruz Biotechnology). The enhanced chemiluminescence system (Amersham-Pharmacia, Buckinghamshire, UK) was used for detection according to the manufacturer's instructions.

Coimmunoprecipitation

COS7 cells were plated in six-well plates at a density of 1.5×10^5 cells/well. Plated cells were transfected with 1 μg of pIRES2-EGFP-*MXI1*-HA, pIRES2-EGFP-*MXI1-0*-HA, or "empty" pIRES2-EGFP and 1 μg of pCS2+MT-mSin3A, using FuGENE 6 at a ratio of 3:1 FuGENE 6 to DNA. Twenty-four hours after transfection, cells were washed with 1 × PBS. Cells were lysed with 275 μl immunoprecipitation (IP) lysis buffer (50 mM Tris-HCl pH 7.4, 150 mM NaCl, 1% NP40, with Complete Mini Protease Inhibitor Cocktail (Roche)) and transferred to cold 1.5-ml microcentrifuge tubes. Lysates were sonicated and centrifuged at >10,000*g* for 10 minutes at 4°C to separate insoluble proteins. The supernatant was transferred to ice-cold tubes and an aliquot was saved as whole cell lysate (WCL). Protein lysates were incubated with 1 μg of immunoprecipitation antibody (anti-HA or anti-Myc for Mxi-Sin3, and anti-HA or anti-FLAG for Mxi-Max) at 4°C rotating for 1 hour. Fifty microliters of protein A/G (1:1) Sepharose (Zymed Laboratories, San Francisco, CA) was added to each reaction and the mixture incubated an additional 2 hours. Immune complexes were pelleted by

centrifugation at 4000 rpm (4°C) and washed four times with IP wash buffer (PBS + 100 mM KCl and 0.25% NP40) before SDS-PAGE and Western blot analysis.

Electrophoretic Mobility Shift Assays

A double-stranded oligonucleotide probe containing the CACGTG Myc/Max binding site was synthesized by heating a pair of complementary oligonucleotide primers (5′-CCCG-ACC ACGTGGTCTGA-3′ and 5′-TCAGACCACGTGGTC-GGG-3′) to 95°C for 10 minutes and then cooling slowly to room temperature. After hybridization, probes were end-labeled with ^{32}P. Purified Max, Mxi1-0, and Mxi1 proteins were prepared from pET-30a(+)-Max, −Mxi1-0, or −Mxi1 transformed BL21(DE3) *E. coli* bacteria (Stratagene) using previously described methods [40]. DNA−protein reactions were performed in gel mobility shift buffer (10 mM Tris−HCl (pH 7.4), 80 mM NaCl, 1 mM dithiothreitol, and 5% glycerol), with purified Max and Mxi1-0 or Mxi1 proteins, 0.25 mg of herring sperm DNA, and 0.5 mg of poly(dI-dC). Reactions were incubated at 42°C for 15 minutes and at 20°C for 15 minutes after adding ^{32}P-labeled probe. Where indicated, anti-Max antibody (Santa Cruz Biotechnology) was then added, and incubation was continued at room temperature for 15 minutes. The DNA−protein complexes were analyzed on a 5% polyacrylamide gel run at 16°C in 0.25 × TBE buffer at 200 V for 2 hours.

Transcription Assays

To assess the effect of Mxi1-0 and Mxi1 on c-Myc−dependent transcription, 1.2 × 10^5 NIH3T3 fibroblasts were cotransfected with 1 μg of pGLDH637Luc (a Myc-responsive, E-box-containing LDH promoter−luciferase reporter plasmid [33]), 100 ng of pRSVMyc (a eukaryotic expression plasmid that constitutively expresses c-Myc under control of the RSV promoter), and 500 ng of either pIRES2-EGFP-*MXI1-0*-HA, pIRES2-EGFP-*MXI1*-HA, or pIRES2-EGFP. Transfections were performed with FuGENE 6, and luciferase assays (Promega) were performed 24 hours after transfection. Initial studies were performed with the Dual-Luciferase assay system, but the presence of even small amounts of *Renilla* luciferase plasmid reduced the baseline firefly luciferase levels, so subsequent transfections were normalized for total protein by the Bradford method. Reactions were performed in triplicate and repeated at least three times; results are expressed as the mean ± SEM.

Tumor and Normal Brain Specimens

RNA was prepared using an RNeasy Kit (Qiagen, Valencia, CA) from frozen specimens obtained from 10 patients with histologically confirmed glioblastoma multiforme, as well as seven normal brain samples obtained from patients who underwent biopsy for nonmalignant conditions. Specimens had been obtained, coded (patient-specific identifiers were stripped), and frozen in liquid nitrogen as part of a University of Michigan human brain tumor bank >5 years previously; there was no possibility to link specimens to individual patients. Approval to analyze specimens was obtained from the University of Michigan Institutional Review Board.

Results

Identification of Mxi1-0, a Novel Mxi1 Isoform, in Human Neuroblastoma

We used the technique of restriction landmark genome scanning [34−36] to perform an unbiased search for expressed genes that are upregulated in the IMR-32 human neuroblastoma cell line [37,38]. A spot on a 2-D gel that was significantly upregulated in these cells was extracted, cloned, and sequenced, and found to be identical to human *MXI1* (h*MXI1*) in its 3′ end, but lost homology at the junction of the first and second exons of h*MXI1* (Figure 1*A*, hMxi1-0). Surprisingly, the sequence of the 5′ end of this cDNA was identical to the 5′ sequence of m*Mxi1-0*, but included 183 additional base pairs of upstream sequence that was similar to available sequence from the 5′ "untranslated" region of m*Mxi1-0*. The human and mouse upstream sequences were 92% (169/183) identical at the nucleotide level (Figure 1*B*), but the h*MXI1-0* sequence included an additional single cytosine base pair in a polyC tract located 80 bp upstream of the previously identified ATG. Of note, the additional cytosine was present in both human and mouse genomic sequences (Figure 1*B*), in contrast to the originally described Shimizu et al. [31] 5′ untranslated m*Mxi1-0* sequence. This "frameshift" relative to m*Mxi1-0* allows for an in-frame upstream ATG start codon that, when translated, encodes 61 additional N-terminal amino acids. This proline-rich region includes consensus motifs for amidation (aa 1−4), myristylation (aa 17−22), and glycosylation (aa 56−59), but there are no other protein homology motifs from the PROSITE database. Specifically, the region contains no known nuclear localization or cytoplasmic retention motifs. The identification of this novel sequence suggested that it might be encoded by an alternative exon distinct from exon 1. Thus, the novel isoform (dubbed "Mxi1-0") shares exons 2 to 6 with hMxi1, but differs from hMxi1 in having an alternative first exon (exon 0 GenBank Accession No. AY576484). Exon 0 aa 62 to 91 are similar (but not identical) to exon 1 aa 1 to 25, and, like exon 1, encode a predicted SID. The human and mouse exon 0 sequences are 95% (259/274) similar at the DNA level (Figure 1*B*) and the encoded amino acids are 93% (84/90) similar (Figure 1*C*).

Localization of Exon 0 Upstream of Exon 1 on Human Chromosome 10 and Mouse Chromosome 19

We obtained a human genomic bacterial artificial chromosome (BAC) clone that contains sequences present in both exon 0 and exon 1, and mapping analysis (by Southern blot after digestion with different restriction enzymes; data not shown) indicated that exon 0 was approximately 20 kb upstream of exon 1 (Figure 2). Subsequent analysis of human chromosome 10 genomic DNA sequence (GenBank Accession No. AL360182) identified the *MXI1* exon 0 sequence 18,088 bp upstream of exon 1, confirming that this sequence represents a distinct exon. Sequence analysis of mouse chromosome 19 (GenBank Accession No. NT_039692) also identified exon 0 approximately 18,996 bp upstream of

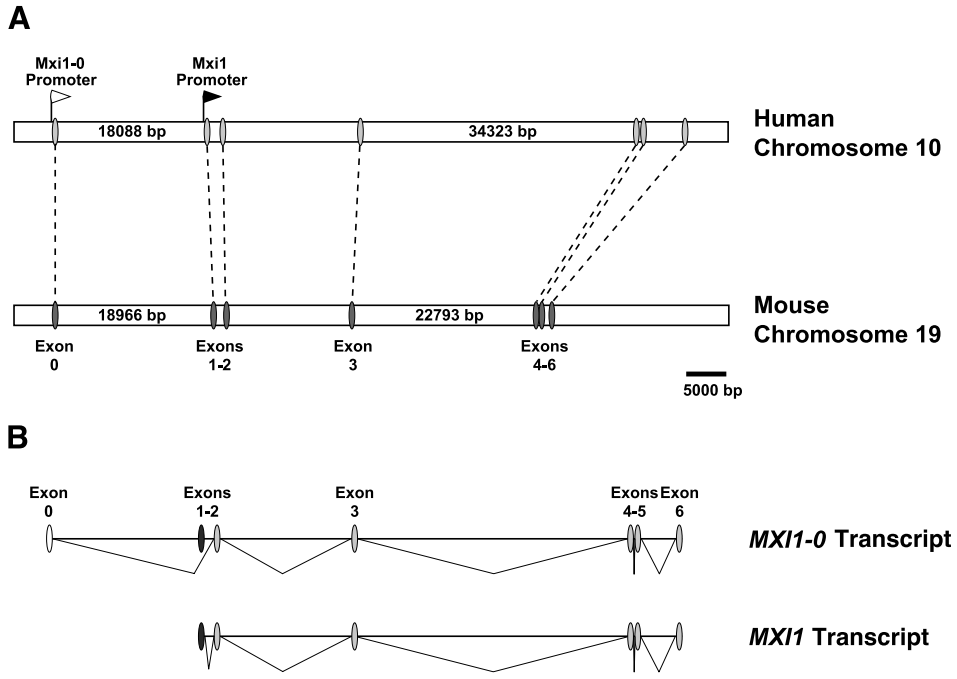

Figure 2. *(A) Genomic organization of human and mouse MXI. Exon 0 lies approximately 19 kb upstream of exon 1. MXI1 mRNA is transcribed from a promoter immediately upstream of exon 1 (filled arrow), whereas MXI1-0 mRNA transcription initiates upstream of exon 0 (open arrow), with splicing out of exon 1. Exons are indicated by shaded ovals, and distances between exons are shown in base pairs. Genomic organization is based on GenBank sequences for human chromosome 10 (GenBank Accession No. AL360182) and mouse chromosome 19 (GenBank Accession No. NT_039692). The actual size of mouse intron 3 is almost certainly greater than indicated here, because the available GenBank sequence contains several N stretches. (B) Derivation of MXI1-0 and MXI1 transcripts. Spliced introns are indicated by diagonal lines. Note that exon 1 is spliced out of the MXI1-0 transcript.*

exon 1 (Figure 2), and illustrates conservation of genomic structure between the human *MXI1* and mouse *mxi1* loci.

Sequences Upstream of Exon 0 Contain a Putative Promoter

If the exon 0 genomic sequence encodes a distinct transcript, sequences upstream of the exon 0 ATG#0 (that presumably regulate its transcription) should demonstrate promoter activity in a luciferase assay. Because we have previously characterized the *MXI1* exon 1 promoter [39], we tested the promoter activity of a luciferase construct containing 1000 bp of putative human *MXI1-0* promoter sequence upstream of the putative exon 0 start codon (ATG#0 in Figure 1*B*). Parallel transfections with *MXI1-0* and *MXI1* promoter constructs showed similar levels of promoter activity (Figure 3*A*) in both U87MG and U373MG glioblastoma cells, and in K562 erythroleukemic cells, indicating inherent *MXI1-0* transcriptional activity in these cell lines. Deletion analysis of putative *MXI1-0* promoter constructs in K562 cells showed promoter activity within 435 bp of sequence upstream of ATG#0, but no activity above background with constructs that include either 145 bp upstream of ATG#0, or 328 bp (= 145 + 183 bp) upstream of ATG#1 (Figure 3*B*). Thus, promoter studies are consistent with the notion that Mxi1-0 is a novel protein whose expression is subject to specific regulation, and suggest that the 183 bp corresponding to the Mxi1-0^{1-61} amino terminal extension is encoded.

Expression of MXI1-0 and MXI1

Northern blot analysis with exon-specific probes was used to compare relative levels of *MXI1-0* and *MXI1* expression in different human tissue types. In contrast to *MXI1*, *MXI1-0* mRNA is expressed more prominently in human fetal tissue (Figure 4*A*). Conversely, *MXI1* is expressed at higher levels in adult human tissues (data not shown).

To analyze relative levels of *MXI1-0* and *MXI1* expression, we developed a multiplex RT-PCR assay, using exon 0– and exon 1–specific forward primers and a common reverse primer in exon 3 (Figure 4*B*). Although the RT-PCR technique is inherently semiquantitative, the use of a common reverse primer, together with the similar product size, permits direct comparison of *MXI1-0* and *MXI1* expression in a given cell or tissue type. Specifically, measuring the ratio of *MXI1-0*/*MXI1* band intensities provides a semiquantitative indication of relative transcript levels within a given sample, and this ratio may be compared between samples. We have detected both *MXI1-0* and *MXI1* transcripts by PCR in cDNA libraries derived from both human and mouse tissues (Figure 4*C*), indicating that both isoforms are coexpressed.

Finally, we determined the intracellular localization patterns of Mxi1-0 and Mxi1. As we [24] and others [41] have observed previously, overexpression of Mxi1 in COS7 cells results in a speckled nuclear expression pattern (Figure 5, *A* and *B*). In contrast, Mxi1-0 appears predominantly in the cytoplasm, with only minimal expression in the nucleus (Figure 5, *C* and *D*). Similar patterns were observed in U87MG glioblastoma cells (data not shown). Thus, in spite

of their similarity, Mxi1-0 and Mxi1 have strikingly different intracellular localization patterns.

Mxi1-0 Interacts With Sin3 and Dimerizes With Max to Recognize E-Box Sequences

The predicted sizes of the translated Mxi1-0 and Mxi1 proteins are 32 and 26 kDa, respectively. This was confirmed by *in vitro* translation using plasmids encoding HA-tagged Mxi1-0 or Mxi1 (Figure 6*A*). We used immunoprecipitation to demonstrate that Mxi1-0, like Mxi1, is able to interact with both Max (Figure 6*B*) and Sin3 (Figure 6*C*). Identical results were obtained with Mxi1 or Sin3 IP pulldowns, indicating that the N-terminal 60 amino acids present in Mxi1-0 does not affect interaction with Sin3 through the SID. Furthermore, like Mxi1, Mxi1-0 interacts with Max and binds to CACGTG-containing DNA sequences in the electrophoretic mobility shift assay (Figure 7). Thus, Mxi1-0 interacts with Sin3 and dimerizes with Max to recognize E-box sequences, indicating that it might have transcriptional regulatory activity.

Mxi1-0 Lacks Significant Transcriptional Repression Activity

The discovery that *MXI1-0* expression is increased in fetal tissues suggested that Mxi1-0 might be associated with proliferation, rather than growth suppression like Mxi1. Thus, we have begun to study the functional activity of Mxi1-0 in comparison with Mxi1. We determined the effect of Mxi1-0 on c-Myc–dependent transcription in a transient transfection assay with an LDH promoter reporter construct that contains two E-box binding sites. Baseline transcription activated by c-Myc was significantly reduced (by 50%) in

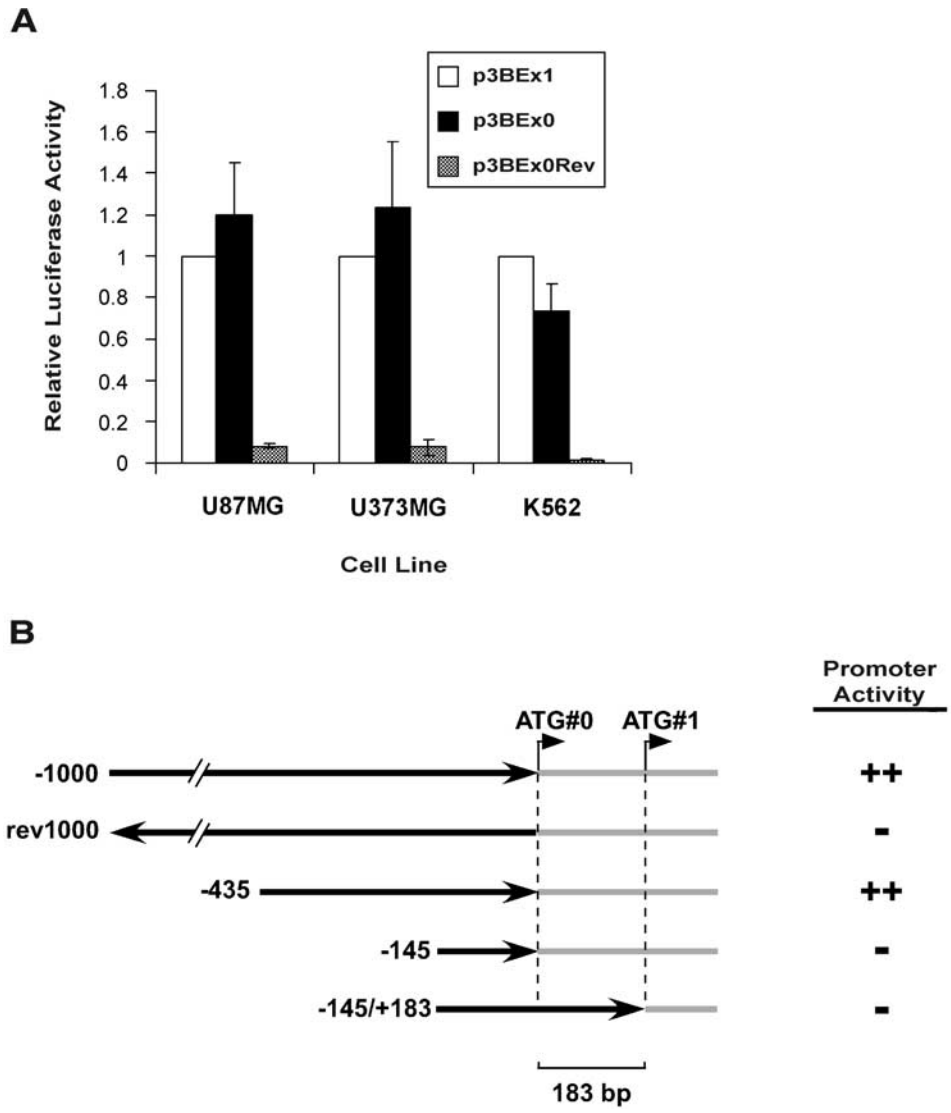

Figure 3. *(A) Exon 0 promoter activity is detectable in different cell lines. Luciferase activity of pGL3Basic-Ex0P (p3BEx0) or pGL3BasicEx0PRev (p3BEx0Rev, the 1-kb exon 0 promoter fragment in reverse orientation) reporter constructs transfected into glioblastoma (U87MG, U373MG) or myeloid leukemia (K562) cells are shown. Luciferase activities are shown relative to pGL3Basic-Ex1P (p3BEx1, 100%), and have been normalized to cotransfected Renilla activities. Each experiment was performed in triplicate a minimum of three times, and error bars indicate standard error of the mean. (B) Deletion analysis of exon 0 promoter. Portions of exon 0 promoter (100, 435, and 145 bp) cloned into pGL3Basic are indicated by solid black arrows, with exon 0 coding sequence shown as gray bars. Positions of ATG#0 and ATG#1 are indicated, with 183 bp of intervening sequence. −145/+183 refers to pGL3Basic construct containing sequence upstream of ATG#1. Relative promoter activity in K562 cells is indicated.*

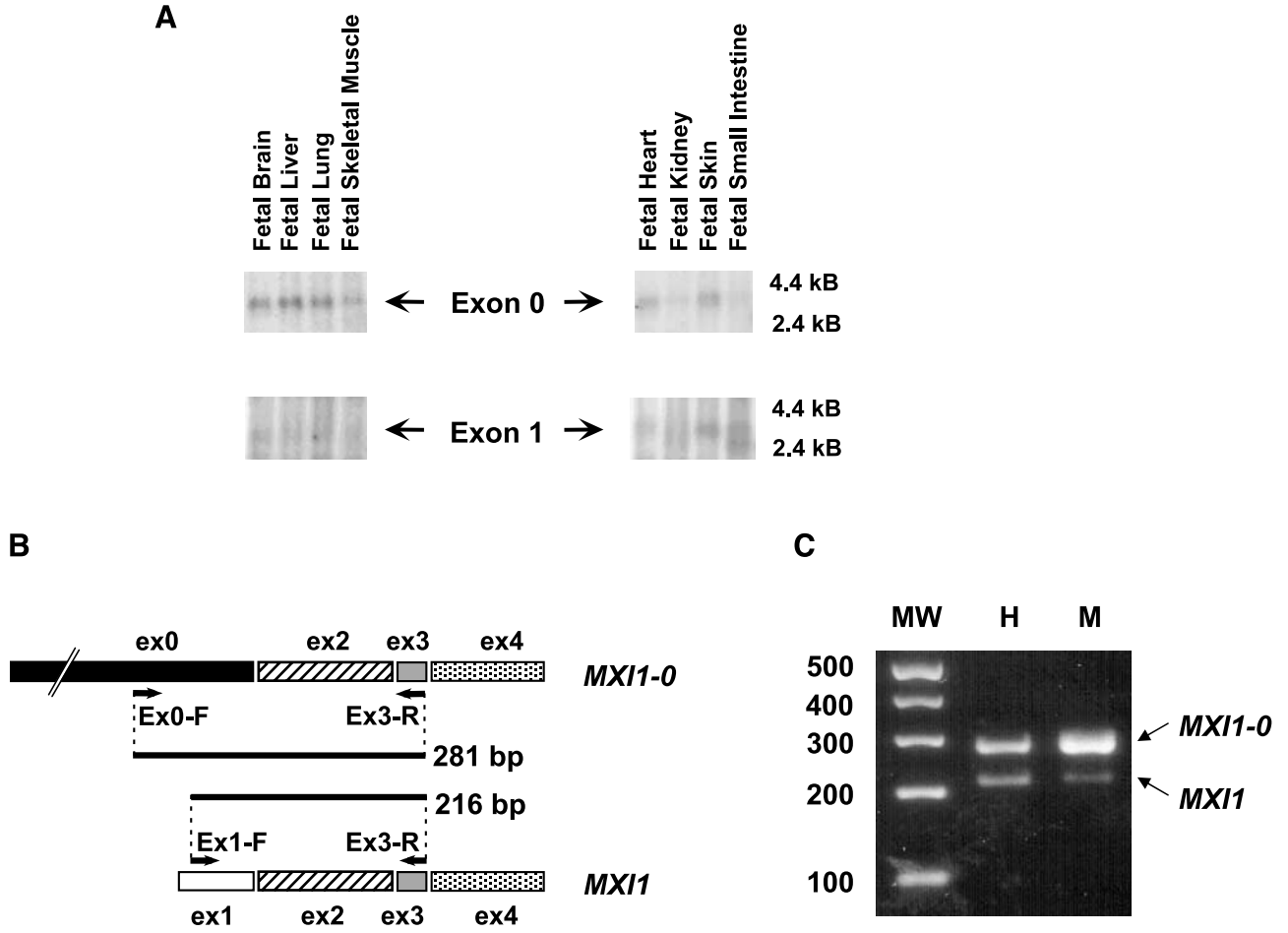

Figure 4. *MXI1-0 and MXI1 expression patterns. (A) MXI1-0 mRNA is preferentially expressed in fetal tissues. REAL Hu Fetal mRNA blots 1 and 2 (BD BioSciences-Clontech) were probed with cRNA probes specific for exon 0 (top panel) or exon 1 (bottom panel). Blots were probed with exon 1 probe first, stripped, then reprobed with exon 0 probe. The expected size of MXI1 mRNA is 2.8 to 3.0 kb (based on previous reports) [6,55] and MXI1-0 mRNA signal is comparable in size. (B) Schematic of multiplex RT-PCR. Solid black bar indicates exon 0, white bar is exon 1, diagonal black striped bar is exon 2, gray bar is exon 3, and dotted bar is exon 4. Forward primers specific for exon 0 (Ex0-F) and exon 1 (Ex1-F) and a common reverse primer from exon 3 (Ex3-R) are used to amplify 281- and 216-bp products, respectively. (C) MXI1-0 and MXI1 are both expressed in both human and mouse cDNA. PCR was performed with MXI1-0– and MXI1-specific forward primers and a common reverse primer, using human heart (H) or mouse pGAB (M) cDNA libraries (gift of G. Nunez). Both MXI1-0 and MXI1 bands are amplified from each cDNA source.*

the presence of Mxi1 in comparison with empty vector (Figure 8). In contrast, Mxi1-0 cotransfection did not significantly affect levels of Myc-dependent transcription. Neither Mxi1-0 nor Mxi1 affected E-box–dependent transcription in the absence of c-Myc (data not shown). These results indicate that Mxi1-0 is unable to repress c-Myc–dependent transcription.

MXI1-0 Is Overexpressed Relative to MXI1 in Glioblastoma Tumors

Because Mxi1-0 does not repress c-Myc–dependent transcription, its coexpression with Mxi1 could antagonize Mxi1-dependent growth suppression. We therefore hypothesized that Mxi1-0 might be overexpressed relative to Mxi1 in tumor cells as compared with normal tissue. We used the multiplex RT-PCR assay to evaluate *MXI1-0* and *MXI1* levels in primary human glioblastoma tumors compared with normal brain tissue. We found that the *MXI1-0*/*MXI1* ratio is elevated in 10 of 10 primary glioblastoma tumors, as compared with normal brain specimens (Figure 9), and also in three glioblastoma tumor cell lines (data not shown). Thus, these studies indicate that *MXI1-0* mRNA transcripts are overexpressed relative to *MXI1* in glioblastoma tumors as compared with normal brain tissue.

Discussion

After the original discovery of human *MXI1* [6], two groups independently described a mouse *mxi1* homolog [19,31]. The amino acid sequence of one form (mMxi1) [19] was essentially identical to human Mxi1 with the exception of minor changes in the C-terminal region (Figure 1). An alternative mouse Mxi1 isoform (referred to here as mMxi1-0 [31]) was identical to mMxi1 in its C terminus, but differed substantially in its N-terminal amino acids (Figure 1). Only a single subsequent reference has been made to m*Mxi1-0* [32]. No specific information related to the functional activity of m*Mxi1-0* has been reported, and the discrepancy between the two mouse *mxi1* forms has not been addressed in the literature. In a search for genes that are upregulated in

human neuroblastoma we have identified human Mxi1-0, and in this report we begin to characterize this alternatively transcribed Mxi1 isoform.

The human Mxi1-0 isoform shares exons 2 to 6 with Mxi1, but differs from Mxi1 in having an alternative first exon (exon 0). Like exon 1, exon 0 encodes a Sin3 interaction domain (aa 62–92); however, exon 0 also encodes 61 additional N-terminal amino acids. Whereas this proline-rich region includes consensus motifs for amidation, myristylation, and glycosylation, there are no other protein homology motifs (responsible for either nuclear localization or cytoplasmic retention) from the PROSITE database. The absence of exon 0 sequence from the intron between h*MXI1* exons 1 and 2 [17] suggested that it was derived from an additional, more upstream, alternative first exon (exon 0) (Figure 2), and examination of both human and mouse GenBank genomic sequences revealed the presence of exon 0 18 to 19 kb upstream of exon 1. Because we have only observed exon 0 juxtaposed to exon 2—and never to exon 1—transcription through the exon 0 promoter must result in the splicing out of exon 1. Exon 0 therefore represents an alternative first exon.

The splicing of alternative first exons to a common set of downstream exons represents a mechanism by which diverse RNAs (and ultimately proteins) can be generated. It has recently been estimated that a large number of human genes (>3000) contain multiple variable first exons [42]. Although most of these genes (~80%) have two alternative first exons, as many as 10 variable first exons have been identified for some genes. Proteins encoded by variable transcripts have been shown to have differences in function [42], different subcellular localization patterns [43], promoter-dependent differential tissue or lineage expression [42], altered posttranscriptional gene regulation through mRNA processing, export, stability, or altered translation potential [44], or modified "native" protein function, resulting in a dominant negative phenotype [45,46]. Although alternative transcripts (derived from distinct promoters or splicing pathways) that encode proteins with distinct functions have been reported for many proliferation-related genes (including c-Myc and Myb [47,48]), our identification of Mxi1-0 represents the first Mad family member derived from an alternative transcript. The presence of an alternative first *MXI1* coding exon raises the possibility that other *MAD* family genes might also harbor alternative first exons. Although sequences homologous to *MXI1* exon 0 are not found upstream of the human *MAD1*, *MAD3*, and *MAD4* genes, these genes might include other alternative upstream exons. It is possible, however, that the alternative *MXI1-0* transcript is unique to the *MXI1* locus. Because *MXI1* is the only *MAD* family gene to date whose inactivation is associated with a tumorigenic phenotype [49,50], the expression of Mxi1-0 may be required for tight regulation of Mxi1 expression.

Our identification of Mxi1-0 reveals an additional, previously unappreciated level of complexity to regulation within the Myc/Max network and prompts speculation about the

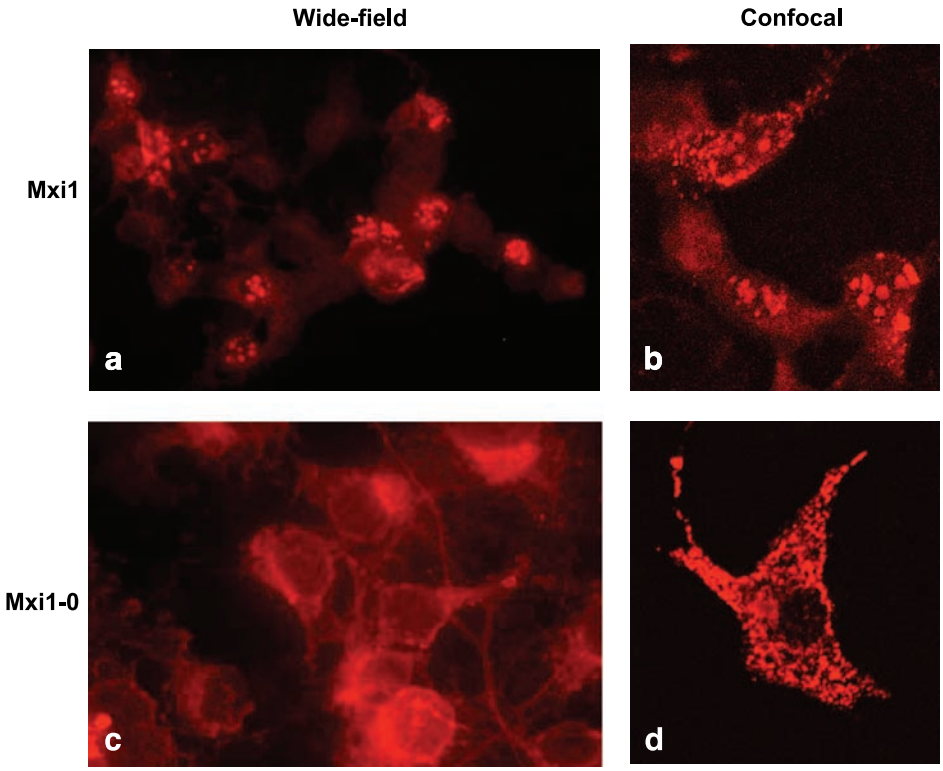

Figure 5. *Intracellular localization of Mxi1 and Mxi1-0. COS7 cells were transiently transfected with pIRES2-EGFP-MXI1-HA (A, B) or pIRES2-EGFP-MXI1-0-HA (C, D), permeabilized, fixed, and then stained with primary rabbit anti–HA antibody followed by Cy3-conjugated secondary goat anti–rabbit antibody. Images shown were taken with wide-field epifluorescence microscopy (A, C, original magnification, × 200) or confocal microscopy (B, D, original magnification, ×500). Note primarily punctuate nuclear distribution of Mxi1, and diffuse cytoplasmic (nonnuclear) expression pattern of Mxi1-0.*

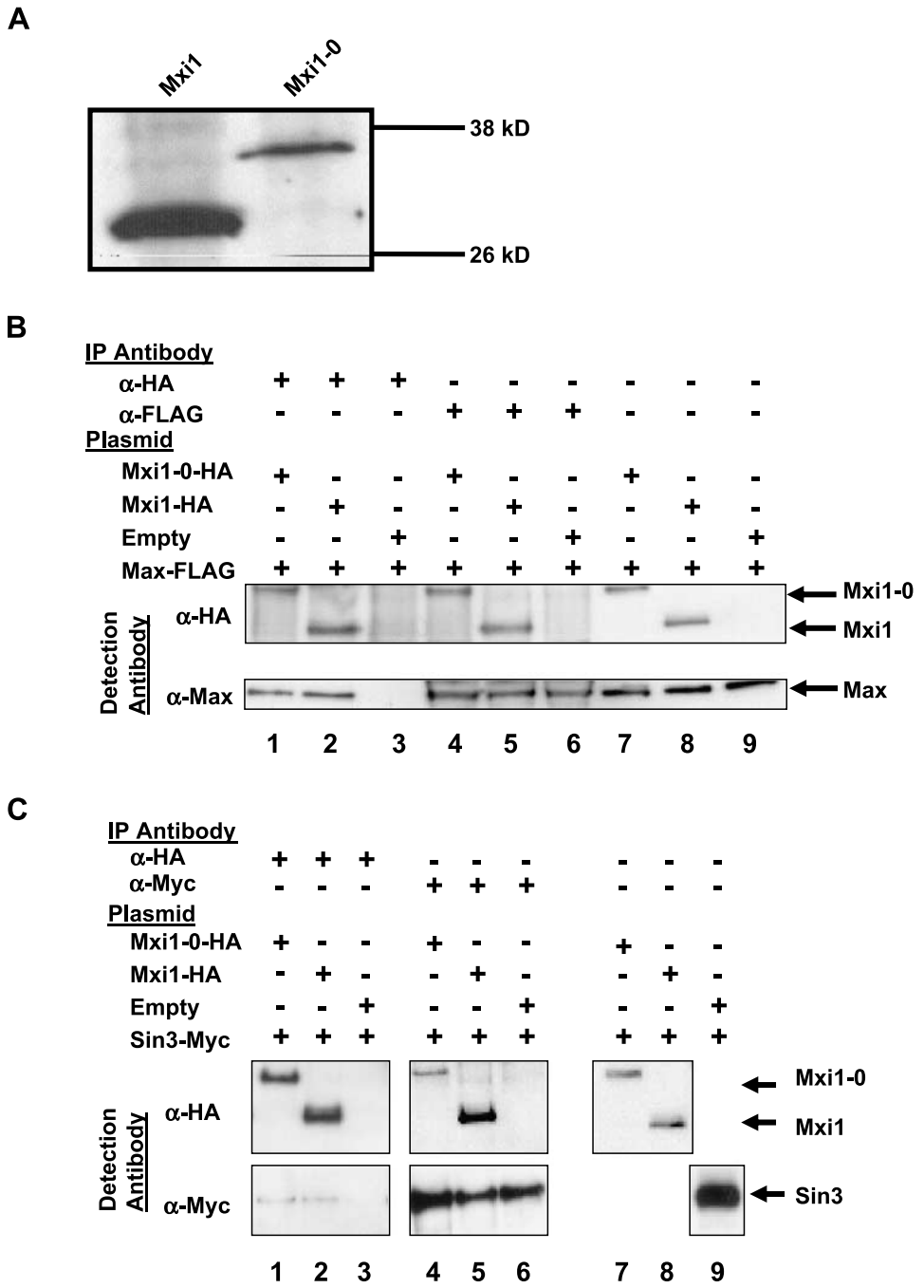

Figure 6. *Mxi1-0 and Mxi1 protein interactions. (A) Expression of Mxi1-0 and Mxi1 proteins. ^{35}S-labeled reticulocyte lysate in vitro transcription/translation of HA-tagged Mxi1-0 and Mxi1 demonstrates translated proteins with the expected size difference. (B) Mxi1-0 and Mxi1 both interact with Max. COS7 cells were transiently transfected with pCMV-Max-YFP-FLAG (lanes 1–9), and pIRES2-EGFP expression vectors for Mxi1-0-HA (lanes 1, 4, and 7), Mxi1-HA (lanes 2, 5, and 8) or empty vector (lanes 3, 6, and 9). Immunoprecipitation (IP) was performed with anti–HA or anti–FLAG antibodies, and after electrophoresis, blots were probed with either anti–HA or anti–Max antibodies. Whole cell lysates (WCLs) that were not subjected to IP (lanes 7–9) contained the expected proteins upon Western blotting. (C) Mxi1-0 and Mxi1 both interact with Sin3. COS7 cells were transiently transfected with a myc-tagged mSin3A expression vector (pCS2+MT-mSin3A, lanes 1–9), and pIRES2-EGFP expression vectors for Mxi1-0-HA (lanes 1, 4, and 7), Mxi1-HA (lanes 2, 5, and 8) or empty vector (lanes 3, 6, and 9). Immunoprecipitation was performed with anti–HA or anti–Myc antibodies, and following electrophoresis, blots were probed with either anti–HA or anti–Myc antibodies. WCLs that were not subjected to IP (lanes 7–9) contained the expected proteins upon Western blotting.*

possible function of Mxi1-0. The ability of Mxi1-0 to interact with Max and with DNA (Figures 6*B* and 7) is not surprising, given the fact that Mxi1-0 and Mxi1 share identical DNA binding and HLH-ZIP domains. The interaction with Sin3 is also expected because the 3′ portion of exon 0 encodes a SID similar to that of Mxi1 and other Mad family members. On this basis, Mxi1-0 would be predicted to synergize with Mxi1 and inhibit Myc activity, and so it is surprising that Mxi1-0 is unable to inhibit Myc-dependent transcription (Figure 8). It is notable, however, that the intracellular expression pattern of Mxi1-0 differs remarkably from that of Mxi1. Whereas Mxi1 exhibits a predominantly speckled nuclear pattern,

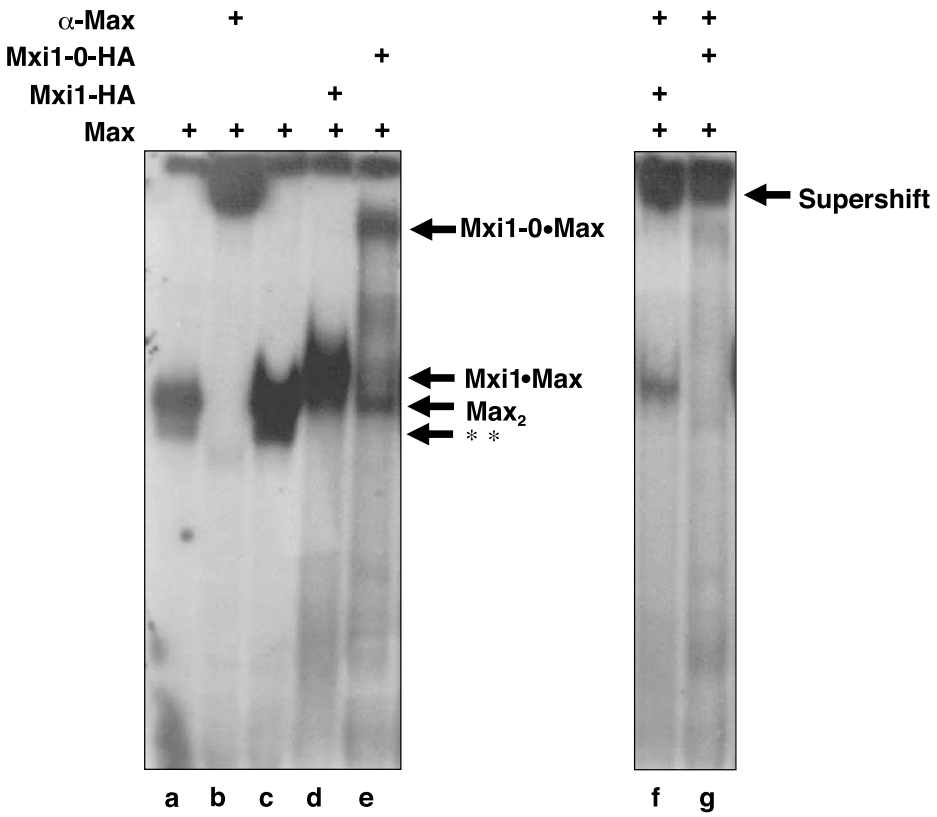

Figure 7. *Mxi1-0-Max and Mxi1-Max both recognize and bind to E-box-containing DNA. Purified 6xHis-Max without (lanes a and c) or with 6xHis-Mxi1 (lanes d and f) or 6xHis-Mxi1-0 (lanes e and g) proteins were mixed together and incubated for 15 minutes at 42° C. A ^{32}P-labeled E-box–containing oligonucleotide probe was added and incubated for 15 minutes at RT. Where indicated, anti-Max antibody was added and incubated for an additional 15 minutes at RT (lanes b, f, and g). The positions of shifted and supershifted band complexes are shown; Max_2 denotes the position of Max–Max homodimers bound to DNA, and ** indicates a less prominent subshifted band seen only with purified Max.*

Mxi1-0 is primarily localized to the cytoplasm (Figure 5). Because Mxi1-0 and Mxi1 differ only in their amino termini, the cytoplasmic localization of Mxi1-0 must be mediated by amino acids in domains encoded by exon 0, most likely within the 61 amino acid N-terminal extension. As a result, even though Mxi1-0 can bind to Sin3 (and potentially mediate histone deacetylase recruitment, chromatin condensation, and transcriptional repression), its predominantly cytoplasmic localization may preclude a transcriptional regulatory role in the nucleus, resulting in the inability of Mxi1-0 to repress Myc-dependent transcription.

Alternatively, because Mxi1-0 includes domains for Sin3 interaction, Max dimerization and DNA binding, it is tempting to speculate that Mxi1-0 may regulate transcription under

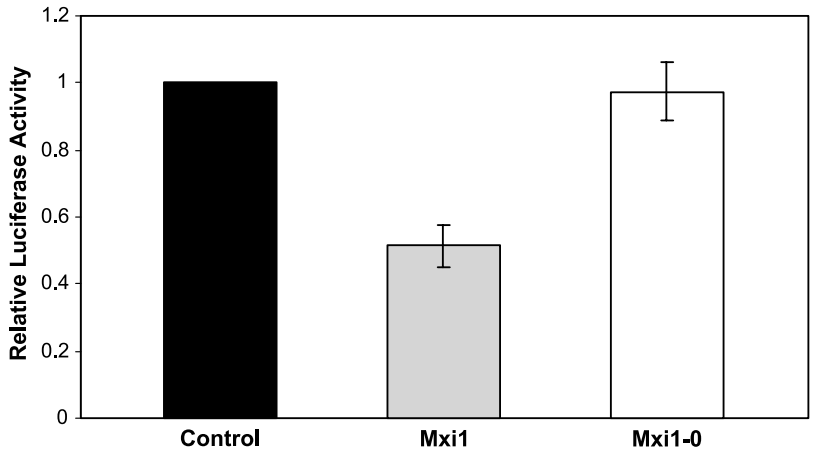

Figure 8. *Mxi1-0 fails to repress Myc-dependent transcription. NIH3T3 cells were cotransfected with an E-box-containing LDH–luciferase reporter plasmid (1 μg), pMLV c-Myc (0.1 μg), and 0.5 μg of empty pIRES2-EGFP vector (control), pIRES2-EGFP-Mxi1 (Mxi1), or pIRES2-EGFP-Mxi1-0 (Mxi1-0). Lysates were prepared after 24 hours; luciferase activity was quantified. The results are standardized to pIG empty control and expressed as the mean (± SEM) of 12 independent experiments in triplicate.*

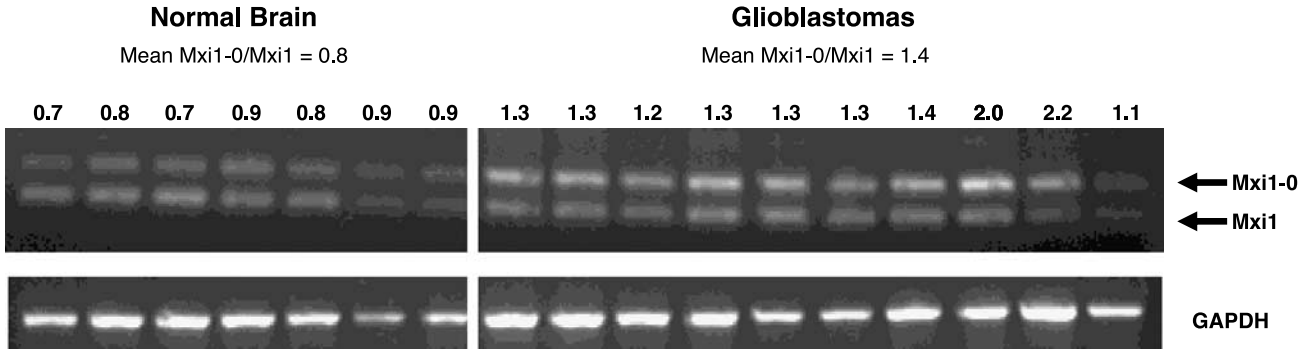

Figure 9. *MXI1-0 is overexpressed in glioblastoma tumors. Semiquantitative multiplex RT-PCR and standard RT-PCR with GAPDH-specific primers was performed with RNA from 7 normal brain specimens and 10 glioblastoma multiforme tumors. The numbers above the ethidium bromide–stained gel indicate the ratio of MXI1-0 to MXI1 band intensity (normalized to GAPDH), with mean MXI1-0/MXI1 (Ex 0/Ex 1) ratio as indicated.*

appropriate circumstances. It is possible that interaction of Mxi1-0 with an as yet undefined cytoplasmic protein prevents Mxi1-0 from appearing in the nucleus. Altered interaction of Mxi1-0 with this putative cytoplasmic protein (as a result of posttranslational modification, e.g., phosphorylation) could then result in translocation of Mxi1-0 to the nucleus with consequent transcriptional repression. This phenomenon has recently been identified for p53 translocation to the nucleus in the context of Parc, a novel cytoplasmic protein [51,52]. Movement of Mxi1-0 from the cytoplasm to the nucleus could therefore quickly and specifically affect Myc transcriptional activity. This possibility is currently being investigated.

At the same time, however, it is also possible that Mxi1-0 antagonizes Mxi1 activity, precisely because of its cytoplasmic localization. Mxi1-0 could compete with Mxi1 for both Max and Sin3, reducing the availability of Max for dimerization and DNA binding and preventing Sin3-dependent transcriptional repression. Cytoplasmic sequestration of Max and/or Sin3 could make these proteins unavailable for interaction in the nucleus with other Myc or Mad family members. Thus, a rapid increase in the relative amount of cytoplasmic Mxi1-0 could abrogate Mxi1 transcriptional repression in dominant negative fashion. This would result in decreased antagonism of Myc function by Mxi1, with a consequent tendency to increased proliferation. It should be noted that other Mxi1 isoforms (e.g., the WR form that lacks a SID [19], or splice variants that are missing exon 3 [53]) could potentially display similar antagonistic effects.

The *MXI1* locus gives rise to distinct mRNA transcripts encoding proteins that appear to have distinct biological activities. In addition, the expression pattern of *MXI1-0* is distinct from that of *MXI1*: whereas mRNAs encoding both isoforms are present in both human and mouse tissues and cell lines, *MXI1-0* is expressed more prominently than *MXI1* in human fetal tissues (Figure 4) and in primary glioblastoma tumors (Figure 9). This differential expression results, at least in part, from a distinct, exon 0–specific promoter. Like the previously characterized *MXI1* promoter region [39], putative *MXI1-0* promoter sequences are active in both glial and hematopoietic cell lines (Figure 3). These putative *MXI1-0* regulatory sequences also contain consensus AP2 binding sites, and preliminary experiments indicate that AP2-dependent regulation of expression through the *MXI1-0* promoter is different from that of *MXI1* (unpublished observations). Based on these observations, we therefore hypothesize that coexpression of Mxi1-0 with Mxi1 modulates the suppressive activity of Mxi1. Depending on the specific circumstances, Mxi1-0 expression may contribute to increased cell proliferation in both ''immature'' and neoplastic cells. Thus, a relative increase in the Mxi1-0/Mxi1 ratio represents a previously unappreciated mechanism by which Mxi1 growth suppression might be modulated.

The localization of the *MXI1* gene to chromosome 10q24–q25, a glioblastoma hotspot, initially suggested that *MXI1* was a candidate tumor suppressor gene in glioblastomas. Although we had previously identified *MXI1* allelic loss in a significant fraction of glioblastoma tumors [23], we and others [25,54] have been unable to identify mutations in any of the six known coding *MXI1* exons in glioblastoma tumor specimens. Interestingly, *MXI1* coding sequence mutations have been identified in several neurofibrosarcoma patients [28]. Furthermore, we were unable to demonstrate methylation of the *MXI1* promoter as a potential mechanism for silencing the remaining *MXI1* allele (manuscript in preparation). The identification of Mxi1-0 suggests an alternative means by which Mxi1 growth suppressive activity might be downregulated. We have shown that *MXI1-0* is overexpressed relative to *MXI1* in 10 of 10 glioblastoma tumors, whereas *MXI1-0* and *MXI1* levels are comparable in 7 normal brain specimens (Figure 9). The consistent observation of relatively increased *MXI1-0* expression in glioblastoma tumor specimens (but not normal brain) raises the intriguing possibility that the presence of Mxi1-0 counteracts the suppressive activity of Mxi1.

The expression of the alternatively transcribed Mxi1-0 isoform raises questions about the interpretation of previous studies that measured *MXI1* mRNA levels by Northern blot/RT-PCR/*in situ* hybridization using probes or primers downstream of exon 1 (e.g., Refs. [6,55–59]). Whereas ectopic expression experiments have clearly indicated a growth-suppressive role for Mxi1 [23–25], studies examining endogenous *MXI1* levels would have necessarily measured levels of both *MXI1* and *MXI1-0*. Since we have demonstrated

substantial levels of both transcripts in a variety of different cell lines, studies that have previously detailed *MXI1* expression patterns now demand reexamination. To begin to address this issue, we have observed that when U937 cells are induced to differentiate with 12-O-tetradecanoylphorbol-13-acetate (TPA) [55], levels of *MXI1-0* and *MXI1* expression exhibit divergent patterns (unpublished observations).

Furthermore, the identification of Mxi1-0 has implications for the phenotype of the published *mxi1* knockout mouse [26]. In this work, the targeting construct was prepared by disrupting *mxi1* exon 2. Because this exon is shared by both Mxi1 and Mxi1-0, the knockout mouse would be expected to be deficient in both isoforms. If Mxi1-0 antagonizes Mxi1, then the effect of inactivating the growth (and potentially tumor) suppressive activity of Mxi1 might be blunted in the ''dual'' knockout. Thus, it is possible that targeted inactivation of only exon 1 might result in a more dramatic tumorigenic phenotype, if Mxi1-0 is still expressed. Studies are ongoing to prepare an *mxi1* exon 1–only knockout mouse.

In summary, we have identified an alternatively transcribed isoform of the Mxi1 growth suppressor. Mxi1-0, transcribed from an alternative upstream exon, is similar to Mxi1 in terms of its ability to interact with Max, Sin3, and E-box–containing DNA. In contrast to Mxi1, Mxi1-0 exhibits a predominantly cytoplasmic expression pattern, fails to repress Myc-dependent transcription, and is expressed at relatively higher levels in glioblastoma tumors. The identification of Mxi1-0 permits an additional level of regulatory control over the activity of the Mxi1 growth suppressor and deepens the complexity of gene regulation by the Mad family. The existence of Mxi1-0 has important implications for previous studies describing both the expression and functional inactivation of Mxi1.

Acknowledgements

We appreciate the constructive input of M. M. Chao, D. Erichsen, A. Walker, S. Wechsler, R. Wechsler-Reya, and B. Wolf. We are grateful to A. Park and M. Clarke for sharing reagents. D. S. W. is supported by NCI grant 1R01CA92171-01 and by C. S. Mott Children's Hospital, The University of Michigan Comprehensive Cancer Center, and the Strokes Against Cancer Foundation. J. L. G. was supported by a fellowship from the American Association of Neurological Surgeons. L. Q. B. was supported by an American Society of Clinical Oncology Young Investigator Award.

References

[1] Eisenman RN (2001). Deconstructing myc. *Genes Dev* **15,** 2023–2030.
[2] Soucek L and Evan G (2002). Myc—is this the oncogene from hell? *Cancer Cell* **1,** 406–408.
[3] Pelengaris S and Khan M (2003). The many faces of c-MYC. *Arch Biochem Biophys* **416,** 129–136.
[4] Levens DL (2003). Reconstructing MYC. *Genes Dev* **17,** 1071–1077.
[5] Ayer DE, Kretzner L, and Eisenman RN (1993). Mad: a heterodimeric partner for max that antagonizes myc transcriptional activity. *Cell* **72,** 211–222.
[6] Zervos AS, Gyuris J, and Brent R (1993). Mxi1, a protein that specifically interacts with max to bind myc-max recognition sites. *Cell* **72,** 223–232.
[7] Hurlin PJ, Queva C, Koskinen PJ, Steingrimsson E, Ayer DE, Copeland NG, Jenkins NA, and Eisenman RN (1995). Mad3 and Mad4: novel Max-interacting transcriptional repressors that suppress c-Myc dependent transformation and are expressed during neural and epidermal differentiation. *EMBO J* **14,** 5646–5659.
[8] Meroni G, Reymond A, Alcalay M, Borsani G, Tanigami A, Tonlorenzi R, Nigro CL, Messali S, Zollo M, Ledbetter DH, et al. (1997). Rox, a novel bHLHZip protein expressed in quiescent cells that heterodimerizes with Max, binds a non-canonical E box and acts as a transcriptional repressor. *EMBO J* **16,** 2892–2906.
[9] Hurlin PJ, Queva C, and Eisenman RN (1997). Mnt, a novel Max-interacting protein is coexpressed with Myc in proliferating cells and mediates repression at Myc binding sites. *Genes Dev* **11,** 44–58.
[10] Hurlin PJ, Steingrimsson E, Copeland NG, Jenkins NA, and Eisenman RN (1999). Mga, a dual-specificity transcription factor that interacts with Max and contains a T-domain DNA-binding motif. *EMBO J* **18,** 7019–7028.
[11] Hurlin PJ, Ayer DE, Grandori C, and Eisenman RN (1994). The max transcription factor network: involvement of Mad in differentiation and an approach to identification of target genes. *Cold Spring Harbor Symp Quant Biol* **59,** 109–116.
[12] Chin L, Liegeois N, DePinho RA, and Schreiber-Agus N (1996). Functional interactions among members of the Myc superfamily and potential relevance to cutaneous growth and development. *J Investig Dermatol Symp Proc* **1,** 128–135.
[13] Luscher B (2001). Function and regulation of the transcription factors of the Myc/Max/Mad network. *Gene* **277,** 1–14.
[14] Zhou ZQ and Hurlin PJ (2001). The interplay between Mad and Myc in proliferation and differentiation. *Trends Cell Biol* **11,** S10–S14.
[15] Shapiro DN, Valentine V, Eagle L, Yin X, Morris SW, and Prochownik EV (1994). Assignment of the human MAD and MXI1 genes to chromosomes 2p12–p13 and 10q24–q25. *Genomics* **23,** 282–285.
[16] Wechsler DS, Hawkins AL, Li X, Jabs EW, Griffin CA, and Dang CV (1994). Localization of the human Mxi1 transcription factor gene (MXI1) to chromosome 10q24–q25. *Genomics* **21,** 669–672.
[17] Wechsler DS, Shelly CA, and Dang CV (1996). Genomic organization of human *MXI1*, a putative tumor suppressor gene. *Genomics* **32,** 466–470.
[18] Ayer DE, Lawrence QA, and Eisenman RN (1995). Mad-Max transcriptional repression is mediated by ternary complex formation with mammalian homologs of yeast repressor Sin3. *Cell* **80,** 767–776.
[19] Schreiber-Agus N, Chin L, Chen K, Torres R, Rao G, Guida P, Skoultchi AI, and DePinho RA (1995). An amino-terminal domain of Mxi1 mediates anti-Myc oncogenic activity and interacts with a homolog of the yeast transcriptional repressor Sin3. *Cell* **80,** 777–786.
[20] Harper SE, Qiu Y, and Sharp PA (1996). Sin3 corepressor function in Myc-induced transcription and transformation. *Proc Natl Acad Sci USA* **93,** 8536–8540.
[21] Rao G, Alland L, Guida P, Schreiber-Agus N, Chen K, Chin L, Rochelle JM, Seldin MF, Skoultchi AI, and DePinho RA (1996). Mouse Sin3A interacts with and can functionally substitute for the amino-terminal repression of the Myc antagonist Mxi1. *Oncogene* **12,** 1165–1172.
[22] Alland L, Muhle R, Hou H Jr, Potes J, Chin L, Schreiber-Agus N, and DePinho RA (1997). Role for N-CoR and histone deacetylase in Sin3-mediated transcriptional repression. *Nature* **387,** 49–55.
[23] Wechsler DS, Shelly CA, Petroff CA, and Dang CV (1997). Mxi1, a putative tumor suppressor gene, suppresses growth of human glioblastoma cells. *Cancer Res* **57,** 4905–4912.
[24] Taj MM, Tawil RJ, Engstrom LD, Zeng Z, Hwang C, Sanda MG, and Wechsler DS (2001). Mxi1, a Myc antagonist, suppresses proliferation of DU145 human prostate cells. *Prostate* **47,** 194–204.
[25] Manni I, Tunici P, Cirenei N, Albarosa R, Colombo BM, Roz L, Sacchi A, Piaggio G, and Finocchiaro G (2002). Mxi1 inhibits the proliferation of U87 glioma cells through down-regulation of cyclin B1 gene expression. *Br J Cancer* **86,** 477–484.
[26] Schreiber-Agus N, Meng Y, Hoang T, Hou H Jr, Chen K, Greenberg R, Cordon-Cardo C, Lee HW, and DePinho RA (1998). Role of Mxi1 in ageing organ systems and the regulation of normal and neoplastic growth. *Nature* **393,** 483–487.
[27] Kawamata N, Park D, Wilczynski S, Yokota J, and Koeffler HP (1996). Point mutations of the Mxil gene are rare in prostate cancers. *Prostate* **29,** 191–193.
[28] Li XJ, Wang DY, Zhu Y, Guo RJ, Wang XD, Lubomir K, Mukai K, Sasaki H, Yoshida H, Oka T, et al. (1999). Mxi1 mutations in human neurofibrosarcomas. *Jpn J Cancer Res* **90,** 740–746.

[29] Raja S, Finkelstein SD, Baksh FK, Gooding WE, Swalsky PA, Godfrey TE, Buenaventura PO, and Luketich JD (2001). Correlation between dysplasia and mutations of six tumor suppressor genes in Barrett's esophagus. *Ann Thorac Surg* **72,** 1130–1135.

[30] O'Hagan RC, Schreiber-Agus N, Chen K, David G, Engelman JA, Schwab R, Alland L, Thomson C, Ronning DR, Sacchettini JC, et al. (2000). Gene-target recognition among members of the Myc superfamily and implications for oncogenesis. *Nat Genet* **24,** 113–119.

[31] Shimizu E, Shirasawa H, Kodama K, Koseki K, Sato T, and Simizu B (1995). Cloning and sequencing of the murine Mxi1 cDNA. *Gene* **152,** 283–284.

[32] Shimizu E, Shirasawa H, Kodama K, Sato T, and Simizu B (1996). Expression, regulation and polymorphism of the mxi1 genes. *Gene* **176,** 45–48.

[33] Shim H, Lewis BC, Dolde C, Li Q, Wu CS, Chun YS, and Dang CV (1997). Myc target genes in neoplastic transformation. *Curr Top Microbiol Immunol* **224,** 181–190.

[34] Hatada I, Hayashizaki Y, Hirotsune S, Komatsubara H, and Mukai T (1991). A genomic scanning method for higher organisms using restriction sites as landmarks. *Proc Natl Acad Sci USA* **88,** 9523–9527.

[35] Hayashizaki Y, Hirotsune S, Okazaki Y, Hatada I, Shibata H, Kawai J, Hirose K, Watanabe S, Fushiki S, Wada S, et al. (1993). Restriction landmark genomic scanning method and its various applications. *Electrophoresis* **14,** 251–258.

[36] Rouillard JM, Erson AE, Kuick R, Asakawa J, Wimmer K, Muleris M, Petty EM, and Hanash S (2001). Virtual genome scan: a tool for restriction landmark-based scanning of the human genome. *Genome Res* **11,** 1453–1459.

[37] Zhu X, Wimmer K, Kuick R, Lamb BJ, Motyka S, Jasty R, Castle VP, and Hanash SM (2002). N-myc modulates expression of p73 in neuroblastoma. *Neoplasia* **4,** 432–439.

[38] Wimmer K, Zhu XX, Rouillard JM, Ambros PF, Lamb BJ, Kuick R, Eckart M, Weinhausl A, Fonatsch C, and Hanash SM (2002). Combined restriction landmark genomic scanning and virtual genome scans identify a novel human homeobox gene, ALX3, that is hypermethylated in neuroblastoma. *Genes Chromosomes Cancer* **33,** 285–294.

[39] Benson LQ, Coon MR, Krueger LM, Han GC, Sarnaik AA, and Wechsler DS (1999). Expression of *MXI1*, a Myc antagonist, is regulated by Sp1 and AP2. *J Biol Chem* **274,** 28794–28802.

[40] Wechsler DS and Dang CV (1992). Opposite orientations of DNA bending by c-Myc and Max. *Proc Natl Acad Sci USA* **89,** 7635–7639.

[41] Yin X, Landay MF, Han W, Levitan ES, Watkins SC, Levenson RM, Farkas DL, and Prochownik EV (2001). Dynamic *in vivo* interactions among Myc network members. *Oncogene* **20,** 4650–4664.

[42] Zhang T, Haws P, and Wu Q (2004). Multiple variable first exons: a mechanism for cell- and tissue-specific gene regulation. *Genome Res* **14,** 79–89.

[43] Cote F, Boisvert FM, Grondin B, Bazinet M, Goodyer CG, Bazett-Jones DP, and Aubry M (2001). Alternative promoter usage and splicing of ZNF74 multifinger gene produce protein isoforms with a different repressor activity and nuclear partitioning. *DNA Cell Biol* **20,** 159–173.

[44] Brown CY, Mize GJ, Pineda M, George DL, and Morris DR (1999). Role of two upstream open reading frames in the translational control of oncogene mdm2. *Oncogene* **18,** 5631–5637.

[45] Ge K, DuHadaway J, Du W, Herlyn M, Rodeck U, and Prendergast GC (1999). Mechanism for elimination of a tumor suppressor: aberrant splicing of a brain-specific exon causes loss of function of Bin1 in melanoma. *Proc Natl Acad Sci USA* **96,** 9689–9694.

[46] Tajiri T, Liu X, Thompson PM, Tanaka S, Suita S, Zhao H, Maris JM, Prendergast GC, and Hogarty MD (2003). Expression of a MYCN-interacting isoform of the tumor suppressor BIN1 is reduced in neuroblastomas with unfavorable biological features. *Clin Cancer Res* **9,** 3345–3355.

[47] Ayoubi TA and Van De Ven WJ (1996). Regulation of gene expression by alternative promoters. *FASEB J* **10,** 453–460.

[48] Mercatante D and Kole R (2000). Modification of alternative splicing pathways as a potential approach to chemotherapy. *Pharmacol Ther* **85,** 237–243.

[49] Foley Kp and Eisenman RN (1999). Two MAD tails: what the recent knockouts of Mad1 and Mxi1 tell us about the MYC/MAX/MAD network. *Biochim Biophys Acta* **1423,** M37–47.

[50] Queva C, McArthur GA, Iritani BM, and Eisenman RN (2001). Targeted deletion of the S-phase-specific Myc antagonist Mad3 sensitizes neuronal and lymphoid cells to radiation-induced apoptosis. *Mol Cell Biol* **21,** 703–712.

[51] Nikolaev AY, Li M, Puskas N, Qin J, and Gu W (2003). Parc: a cytoplasmic anchor for p53. *Cell* **112,** 29–40.

[52] Nikolaev AY and Gu W (2003). PARC: a potential target for cancer therapy. *Cell Cycle* **2,** 169–171.

[53] Kawamata N, Sakajiri S, Sugimoto K-J, and Koeffler HP (2003). Alternative isoforms of the Mxi1 gene are expressed in hematological cell lines and normal bone marrow. *Blood* **102,** 203.

[54] Fults D, Pedone CA, Thompson GE, Uchiyama CM, Gumpper KL, Iliev D, Vinson VL, Tavtigian SV, and Perry WL III (1998). Microsatellite deletion mapping on chromosome 10q and mutation analysis of MMAC1, FAS, and MXI1 in human glioblastoma multiforme. *Int J Oncol* **12,** 905–910.

[55] Larsson LG, Pettersson M, Oberg F, Nilsson K, and Luscher B (1994). Expression of mad, mxi1, max and c-myc during induced differentiation of hematopoietic cells: opposite regulation of mad and c-myc. *Oncogene* **9,** 1247–1252.

[56] Delgado MD, Lerga A, Canelles M, Gomez-Casares MT, and Leon J (1995). Differential regulation of Max and role of c-Myc during erythroid and myelomonocytic differentiation of K562 cells. *Oncogene* **10,** 1659–1665.

[57] Dooley S, Wundrack I, Blin N, and Welter C (1995). Coexpression pattern of c-myc associated genes in a small cell lung cancer cell line with high steady state c-myc transcription. *Biochem Biophys Res Commun* **213,** 789–795.

[58] Meinhardt G and Hass R (1995). Differential expression of c-myc, max and mxi1 in human myeloid leukemia cells during retrodifferentiation and cell death. *Leuk Res* **19,** 699–705.

[59] Wang Y, Toury R, Hauchecorne M, and Balmain N (1997). Expression and subcellular localization of the Myc superfamily proteins: c-Myc, Max, Mad1 and Mxi1 in the epiphyseal plate cartilage chondrocytes of growing rats. *Cell Mol Biol* **43,** 175–188.